Pharm Res (2011) 28:1723–1732
DOI 10.1007/s11095-011-0408-7

RESEARCH PAPER

Enhanced Stability and Knockdown Efficiency of Poly(ethylene glycol)-*b*-polyphosphoramidate/siRNA Micellar Nanoparticles by Co-condensation with Sodium Triphosphate

Masataka Nakanishi • Rajesh Patil • Yong Ren • Rishab Shyam • Philip Wong • Hai-Quan Mao

Received: 19 December 2010 / Accepted: 21 February 2011 / Published online: 9 March 2011

ABSTRACT

Purpose Polyelectrolyte complex nanoparticles are a promising vehicle for siRNA delivery but suffer from low stability under physiological conditions. An effective stabilization method is essential for the success of polycationic nanoparticle-mediated siRNA delivery. In this study, sodium triphosphate (TPP), an ionic crosslinking agent, is used to stabilize siRNA-containing nanoparticles by co-condensation.

Methods siRNA and TPP were co-encapsulated into a block copolymer, poly(ethylene glycol)-*b*-polyphosphoramidate (PEG-*b*-PPA), to form ternary nanoparticles. Physicochemical characterization was performed by dynamic light scattering and gel electrophoresis. Gene silencing efficiency in cell lines was assessed by dual luciferase assay system.

Results The PEG-*b*-PPA/siRNA/TPP ternary nanoparticles exhibited high uniformity with smaller size (80–100 nm) compared with PEG-*b*-PPA/siRNA nanoparticles and showed increased stability in physiological ionic strength and serum-containing medium, due to the stabilization effect from ionic crosslinks between negatively charged TPP and cationic PPA segment. Transfection and gene silencing efficiency of the TPP-crosslinked nanoparticles were markedly improved over PEG-*b*-PPA/siRNA complexes in serum-containing medium. No significant difference in cell viability was observed between nanoparticles prepared with and without TPP co-condensation.

Conclusions These results demonstrated the effectiveness of TPP co-condensation in compacting polycation/siRNA nanoparticles, improving nanoparticle stability and enhancing the transfection and knockdown efficiency in serum-containing medium.

KEY WORDS block copolymer gene carrier · siRNA · sodium triphosphate · stabilization · ternary nanoparticles

INTRODUCTION

Small interfering RNA (siRNA) has been recognized as a powerful therapeutic agent for effectively silencing a specific gene on a post-transcriptional level (1–3). Many siRNA targets and RNA interference (RNAi) strategies have been devised as a therapeutic approach in the treatment of diseases such as macular degeneration, hepatitis C infection, and cancer (4,5). In spite of several recent successful reports (6), therapeutic application of siRNA has been hampered by limited stability within physiological fluids

Masataka Nakanishi and Rajesh Patil contributed equally to this work.

M. Nakanishi • R. Patil • Y. Ren • H.-Q. Mao
Department of Materials Science and Engineering
Johns Hopkins University
Baltimore, Maryland 21218, USA

M. Nakanishi • H.-Q. Mao
Translational Tissue Engineering Center, Johns Hopkins University
Baltimore, Maryland 21218, USA

R. Shyam
Department of Biomedical Engineering, Johns Hopkins University
Baltimore, Maryland 21218, USA

P. Wong
Department of Neuroscience, Johns Hopkins University
Baltimore, Maryland 21218, USA

H.-Q. Mao
Whitaker Biomedical Engineering Institute, Johns Hopkins University
Baltimore, Maryland 21218, USA

H.-Q. Mao (✉)
101E Maryland Hall, 3400 North Charles Street
Baltimore, Maryland 21218, USA
e-mail: hmao@jhu.edu

and inefficient cell membrane permeation due to high density of negative charge in naked siRNA (7,8). Therefore, development of carriers for efficient siRNA delivery has emerged as a key issue in siRNA therapeutics (9,10). Recent studies have successfully demonstrated that siRNA carriers based on various cationic polymers, lipids and peptides have been used to form nanosized polyplex with siRNA (11,12). However, these polycation/siRNA nanoparticles exhibit poor stability in buffers at physiological ionic strength or in serum-containing media due to the small molecular weight of siRNA chains (13,14). In order to improve the compaction ability and stability of siRNA-containing nanoparticles, several strategies for *in vivo* siRNA delivery have already been proposed, including siRNA conjugates with cholesterol or proteins, and the incorporation of siRNA into polymeric micelles and micro/nanogels (15,16). Huang *et al.* have shown that lipid-coated calcium phosphate nanoparticles could enhance intracellular delivery of siRNA (17). Further modifications such as cross-linking have been developed to stabilize polycation/siRNA nanoparticles in order to achieve high level of transfection. For example, Kataoka *et al.* have demonstrated increased stability of siRNA nanoparticles by cross-linking the core through disulfide bonds to increase the complex stability under physiological salt conditions (18).

We previously reported that the condensation of DNA by block copolymer, poly(ethylene glycol)-*b*-polyphosphoramidate block copolymer (PEG-*b*-PPA), yielded the self-assembled micellar nanoparticles with a complex core surrounded by a PEG corona (19,20). The advantages of these micellar nanoparticles include smaller and more uniform size, improved colloidal stability in serum-containing media, higher protection of incorporated DNA against enzymatic degradation, and prolonged blood circulation (21,22). Despite the success of mediating DNA delivery, PEG-*b*-PPA condensed micelles with siRNA suffered from low stability in salt solution, which may be due to the short and rigid structure of siRNA in contrast to plasmid DNA (13).

Here we report a new method to stabilize polycation/siRNA nanoparticles with sodium triphosphate (TPP) via ionic crosslinking (Fig. 1). TPP was first used to prepare chitosan nanoparticles by forming ionic crosslinks between positively charged amino groups of chitosan and negatively charged phosphates in TPP (23,24). TPP is popular for chitosan crosslinking because of its non-toxic nature and effective crosslinking ability (25,26). We hypothesized that similar crosslinking can form between TPP and positive-charged gene carriers, thus facilitating condensation with siRNA and increasing stability of nanoparticles. In this paper, the stability of nanoparticles with TPP-crosslinked core and the release profile of free siRNA from nanoparticle through an exchange reaction by polyanion were analyzed. Furthermore, the gene knockdown efficiency of PEG-*b*-PPA/siRNA nanoparticles stabilized by TPP was assessed in HeLa and D407 cells *in vitro*.

MATERIALS AND METHODS

Reagents

Sodium triphosphate (TPP) and poly(vinyl sulfate) potassium salt (PVSK) were purchased from Sigma-Aldrich Chemical Co. Ltd. (Milwaukee, WI, USA). WST-1 was purchased from Roche (Penzberg, Germany). UltraPure™ DNase/RNase-Free Distilled Water, Dulbecco's Modified Eagle's Medium (DMEM), Opti-MEM™ and Lipofectamine2000™ were purchased from Invitrogen (Carlsbad, CA, USA). Dual-luciferase reporter assay system and pGL3-control and pRL-CMV vectors were purchased from Promega (Madison, WI, USA). The siRNA was purchased from Ambion (Austin, TX, USA). Formvar-coated carbon grid was purchased from Electron Microscopy Sciences (Hatfield, PA, USA). The sequences of siRNA against *Photinus pyralis* luciferase were as follows: sense 5′-CUUACGCUGAGUACUUCGAdTdT-3′, antisense 5′-UCGAAGUACUCAGCGUAAGdTdT-3′.

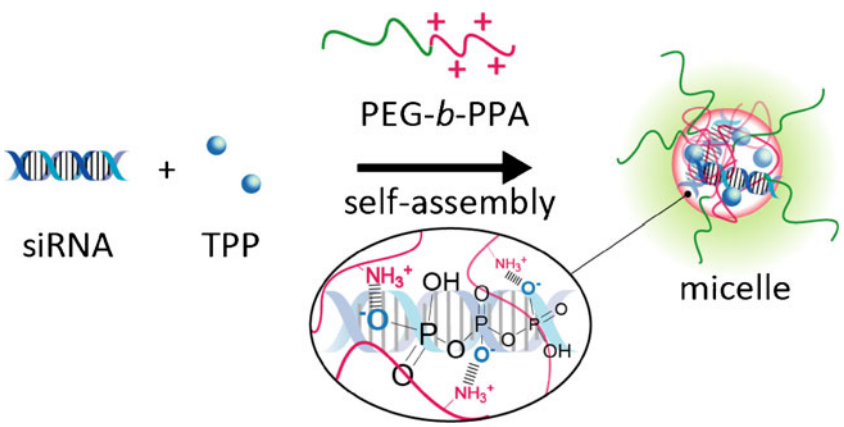

Fig. 1 Schematic of preparation of PEG-*b*-PPA/siRNA/TPP ternary micellar nanoparticles formed through ionic crosslinking with sodium triphosphate (TPP).

Preparation of Nanoparticle with TPP-Crosslinked Core

PEG-*b*-PPA (molecular weights: PEG, 12 kDa, PPA, 38 kDa) was prepared as described in the previous report (19). Ten μL of 4 μM siRNA solution (10 mM Tris–HCl, pH 7.4) was mixed with 10 μL of TPP solution (10 mM Tris–HCl, pH 7.4), followed by the addition of 20 μL of PEG-*b*-PPA solution (10 mM Tris–HCl, pH 7.4) into the mixture of siRNA and TPP solution at different mixing ratios. They were mixed by pipetting, followed by gentle vortex and spin-down. These particles were then incubated at room temperature for 1 h before use or further analysis. The mixing ratio for each formation was determined by N/P and P′/N: [primary amino group of PPA]/[phosphate group of siRNA] and [phosphate group of TPP]/[primary amino group of PPA], respectively. The negative charge number of TPP is defined as three in this study according to the report (27).

Measurement of Size and ζ-potential of Nanoparticles

Mean particle hydrodynamic diameter (*z*-average) and ζ-potential of the nanoparticles were determined by photon correlation spectroscopy and laser Doppler anemometry, respectively, using Zetasizer Nano ZS90 (Malvern Instruments, Malvern, UK) equipped with a He-Ne laser ($\lambda = 633$ nm) as the incident beam. Size distributions were determined by cumulate and histogram analysis, and results are shown as the *z*-averaged size (cumulate mean) with polydispersity index (PDI) (defined in the ISO standard document 13 321:1996). All samples were equilibrated to the defined temperature for 1 h prior to measurement. The ζ-potential values of the complexes were measured in 10 mM Tris–HCl buffer (pH 7.4) containing 150 mM NaCl at 37°C. All samples were equilibrated to the defined temperature for 1 h prior to measurement.

Stability of Nanoparticles in the Physiological Ionic Strength

The effect of crosslinking on nanoparticle stability in buffers with the physiological ionic strength was determined using the Zetasizer Nano ZS90 (Malvern Instruments). The assay was performed by measuring the size and scattering light intensity (SLI) of nanoparticles after 24 h of incubation at 37°C in solutions containing 150 mM of NaCl concentration.

Transmission Electron Microscopy

An aliquot of 10 μL of nanoparticle solution was added to a formvar carbon TEM grid and incubated for 5 min at room temperature, followed by washing with deionized water. The grid was further stained with 2% of uranyl acetate solution and washed with deoinized water twice. Transmission electron microscopy was carried out on Tecnai™ 12 (FEI Company, OR, USA) run at 100 kV.

Gel Retardation Assay

The incorporation of siRNA into nanoparticle assemblies was determined by electrophoresis on a 0.8% agarose gel. Electrophoresis was carried out at a constant voltage of 90 V for 0.5 h in TAE buffer (4.45 mM Tris-acetic acid containing 1.7 mM sodium acetate, pH 8.3). The band of migrated siRNA was visualized under a UV transilluminator (UVP, Upland, CA) at a wavelength of 365 nm after soaking the gel in distilled water containing ethidium bromide (EtBr) (0.5 μg/mL).

Stability of Encapsulated siRNA in Serum-Containing Medium

The siRNA-incorporated nanoparticles were incubated at 37°C with 50% final concentration of fetal bovine serum (FBS) for 1 and 4 h, respectively. Samples were then incubated in 10 μL of 50 mM EDTA for 5 min and 10 μL of 10 mM PVSK was added to displace siRNA from the nanoparticles. The released siRNA was analyzed by electrophoresis on a 20% polyacrylamide gel prepared in 7 M urea and TBE buffer (0.089 M Tris base, 0.089 M boric acid, and 2 mM sodium EDTA, pH 8.3). Polyacrylamide–urea gel (20%) was used due to its high efficiency in separating small fragments of possibly degraded siRNA. Electrophoresis was then carried out with 1× TBE buffer at a constant voltage of 100 V for 1 h. The siRNA bands were visualized under a UV transilluminator after staining for 40 min with a 1:10,000 dilution of SYBR-Green II RNA gel stain (Molecular Probes) in RNase-free water.

Polyanion-Exchange Analysis

Self-assembled nanoparticles prepared above were incubated with in 10 mM Tris–HCl, pH 7.4 at [sulfonate of PVSK]/[phosphate of siRNA] ratio of 5 at 37°C for 5 h. The released siRNA from nanoparticles was analyzed at 1 and 5 h by the gel retardation assay under the same conditions as described above.

Knockdown Efficiency by Nanoparticles and Cell Viability

HeLa cells (human epithelial cervical cancer cell line) and D407 cells (human retinal pigment epithelial cell line) were seeded onto 24-well culture plates at a density of 5×10^4 cells per well in 500 μL of medium, followed by 20 h of

incubation in DMEM containing 10% fetal bovine serum (FBS) without antibiotics. Then, 720 ng/well pGL3-control plasmid encoding *Photinus pyralis* luciferase (P-Luc) and 80 ng/well pRL-CMV plasmid encoding *Renilla reniformis* luciferase (R-Luc) were co-transfected to the cells with Lipofectamine2000™ according to the manufacturer's instructions; cells were further incubated for 4 h. For nanoparticle-transfection groups, the medium was replaced with fresh serum-free medium or medium with 10% FBS, and nanoparticles containing siRNA (100 nM) against P-Luc with or without TPP crosslinking were applied to each well and incubated for 4 h. The medium was then replaced with complete media containing 10% serum, followed by incubation at 37°C with a 5% of CO_2atm. After 44 h, cells were rinsed with PBS and subjected to a luciferase expression assay using the Dual-Luciferase Reporter Assay System. For each assay, P-Luc and R-Luc luminescence was measured using FLUOstar OPTIMA plate reader (BMG LABTECH, Germany) after the addition of appropriate substrates. P-Luc activities were normalized by R-Luc activities, and values are expressed as a ratio to the control value (mean ± SD, $n=4$). Cell viability was determined using WST-1 according to the manufacture's protocol. Incubation conditions were identical to those used in the transfection protocol.

RESULTS

Preparation of PEG-*b*-PPA/siRNA Nanoparticles and Stabilization with TPP

In order to test whether TPP co-condensation enhances the nanoparticle formation, we prepared PEG-*b*-PPA/siRNA nanoparticles with TPP added to the siRNA solution. PEG-*b*-PPA solutions were incubated with a mixture of siRNA and TPP at N/P ratios of 4 and 8 and a variety of P′/N ratios of 0 to 1 to form polyelectrolyte complexes (Fig. 2). In the absence of TPP (P′/N=0), there is no distinct particle formation for N/P ratios of both 4 and 8, where the measured *z*-average size was less than 10 nm with large PDI (Fig. 2a and b). On the other hand, when TPP was used during the condensation, nanoparticle formation was observed at P′/N ratio of 0.1 or higher. The mean particle size of the assembled nanoparticles with TPP-co-condensation increased to 80 to 100 nm as measured by DLS (Fig. 2a and b). Of interest, PDI of nanoparticles prepared with TPP was less than 0.1, and the histogram analysis showed unimodal size distribution. These data indicated that TPP was highly effective in facilitating siRNA condensation and nanoparticle formation.

Significant differences in particle morphology were also observed in transmission electron microscopy (TEM) analysis between nanoparticle preparations in the presence and absence of TPP. TEM images of nanoparticles prepared with TPP showed that these particles were mostly spherical with diameters ranging from 80 to 100 nm (Fig. 2c), corroborating well with the average size (98.2± 10.2 nm) measured by DLS method. On the other hand, the TEM images of particles formed without TPP revealed aggregates with irregular shape and sized ranged from 20 to 100 nm, correlating with higher PDI. Nanoparticles with TPP showed much higher contrast than that without TPP in TEM images, indicating that the TPP-condensed nanoparticles may have more compact polyplex core than that without TPP.

As shown in Fig. 2d, the ζ-potential values of nanoparticles prepared at different P′/N ratios varied significantly and appeared to be highly dependent on P/N ratio. The ζ-potential values decreased sharply from +15 to −1.5 mV when the P′/N ratio increased from 0.1 to 1.0. The near electrostatic neutrality of the particle surface at P′/N ratio of 0.5 to 1.0, with a PEG corona, may be advantageous in preventing nanoparticle aggregation when applied in physiological media.

Complex Stability of Nanoparticles in Salt Solution with Physiological Ionic Strength

The complex stability of nanoparticles was assessed by monitoring changes in size and PDI in 0.15 M of NaCl solution. No dynamic scattering signals were detected for nanoparticles prepared without TPP (P′/N=0) at N/P ratio of 4 or 8 after they were incubated with 0.15 M NaCl solution, due to the charge screening effect. Nanoparticles prepared with lower P′/N ratios (0.1 and 0.2) showed increased sizes after incubating in 0.15 M NaCl. In contrast, nanoparticles prepared at higher P′/N ratios only showed slightly increased particle sizes (average size of 110 and 100 nm for N/P of 4 and 8, respectively) and low PDIs (Fig. 2a and b). This indicates that TPP-crosslinked nanoparticles could stabilize siRNA nanoparticles in a solution with physiological ionic strength.

Nanoparticle Stability in the Presence of 50% Bovine Serum

To test whether the encapsulated siRNA showed improved stability in serum containing medium, nanoparticles were incubated with 50% of fetal bovine serum (FBS) at 37°C followed by gel electrophoresis to analyze the integrity of siRNA. Figure 3 showed that siRNA incubated with 50% FBS was significantly degraded. On the other hand, siRNA recovered from nanoparticles only showed trace amount of degradation for all N/P and P′/N ratios. The siRNA recovered from nanoparticles with and without TPP were

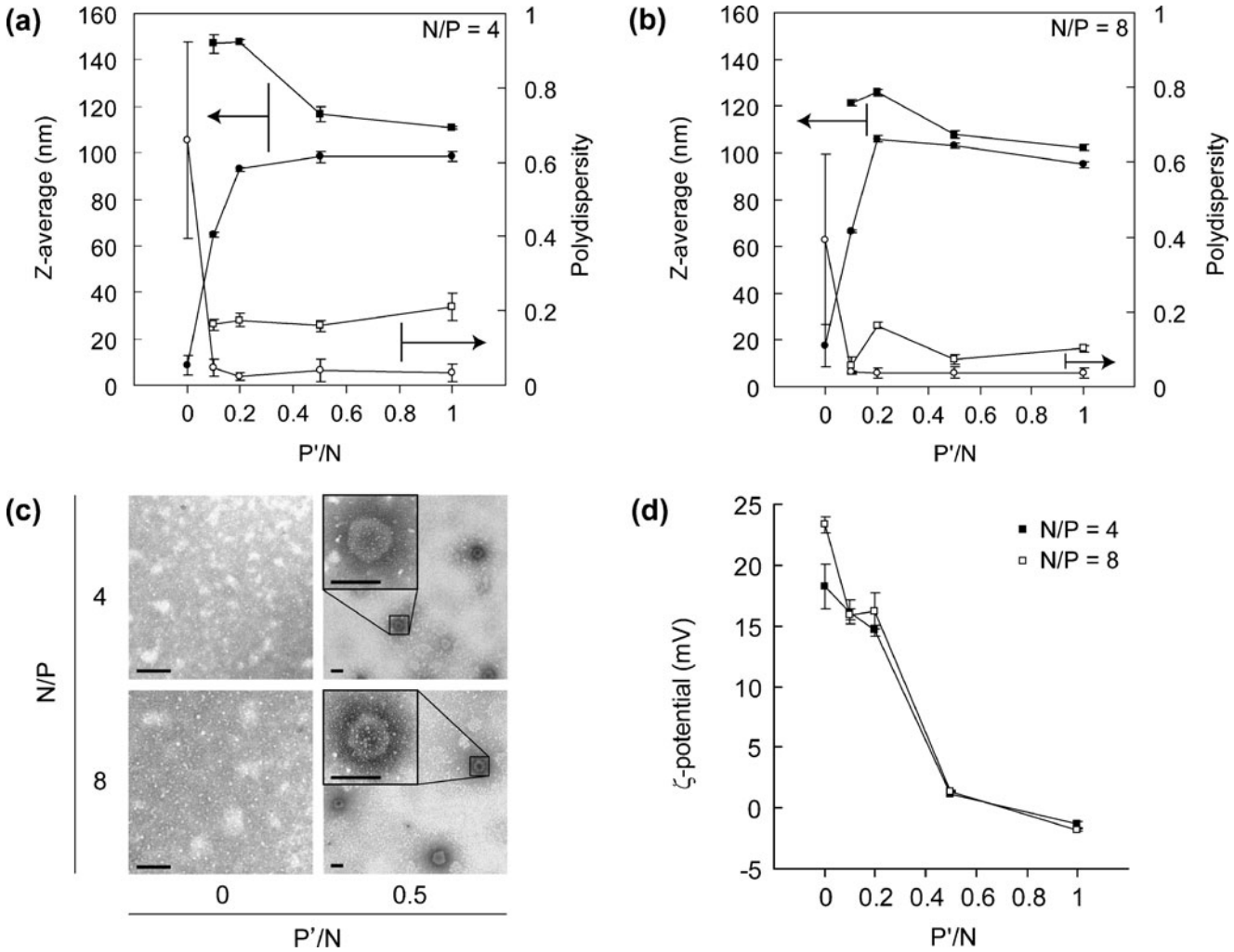

Fig. 2 The *z*-average (*left ordinate*) and PDI (*right ordinate*) measured by dynamic light scattering analysis of nanoparticles formed at various P′/N ratios and N/P ratios of 4 (**a**) and 8 (**b**), respectively, before (*filled circle*, *empty circle*) and after (*filled square*, *empty square*) incubation with 150 mM NaCl for 24 h. Values represent Mean ± SEM ($n = 3$). Particles without TPP crosslinking dissociated after incubation in 150 mM NaCl; therefore, no data points were included for P′/N = 0 for salt incubation lines (*filled square*, *empty square*) here. (**c**) TEM images of nanoparticle formed at P′/N ratios of 0 and 0.5 for N/P ratios of 4 and 8, respectively. Scale bar = 100 nm. (**d**) Zeta-potential of nanoparticles prepared at various P′/N ratios for N/P ratios of 4 (*filled square*) and 8 (*empty square*), respectively. Values represent Mean ± SEM ($n = 3$).

still more intact for 4 h at all the P′/N ratios. No significant difference on siRNA integrity in 50% FBS was observed between nanoparticles prepared with and without TPP. PEG-*b*-PPA/siRNA nanoparticles without TPP showed similar resistance of siRNA to enzymatic degradation for 4 h of incubation with 50% serum as compared to nanoparticles with TPP.

Complex Stability of Nanoparticles Against Challenges with Polyanions

The encapsulation efficiency of siRNA into nanoparticles was confirmed by agarose gel electrophoresis (Fig. 4a and d). Free siRNA was not observed for all samples including the complexes prepared with or without TPP, highlighting the good siRNA condensation ability of PEG-*b*-PPA. More importantly, the complexation ability was not compromised by the addition of TPP at all P′/N ratios tested. In combining with the DLS analysis (Fig. 2a and b), these data indicated that complexation between PEG-*b*-PPA and siRNA was strong enough to inhibit the gel migration ability of siRNA at both N/P ratios of 4 and 8, but distinct particle formation was observed only with TPP-assisted condensation.

The stability of the nanoparticles was also analyzed by characterizing the release profile of incorporated siRNA using a polyanion-exchange reaction (Fig. 4b, c, e, and f) (28,29). There exist various types of anionic polymers, including anionic proteins, sulfated polysaccharides, nuclear chromatin and messenger RNA (mRNA), as essential

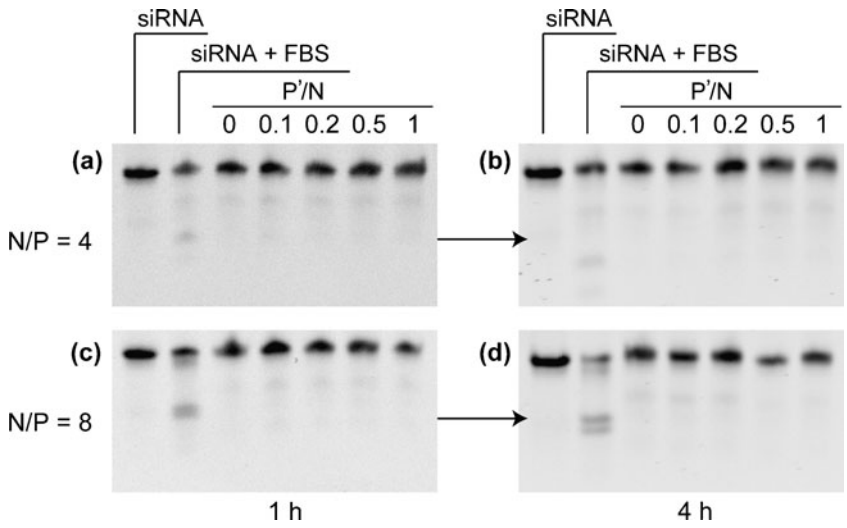

Fig. 3 Gel retardation assay of siRNA integrity in nanoparticles against enzymatic degradation in 50% FBS. Nanoparticles prepared at various conditions were incubated in 50% FBS for 1 h (**a** and **c**) and 4 h (**b** and **d**), respectively.

cellular components. Exchange reaction of polycations with these negatively charged polymers may take place in biological environment. As a result, siRNA may be released from nanoparticles through the intermolecular exchange and facilitate a series of subsequent RNAi processes for gene silencing. On the other hand, nanoparticles should be sufficiently stable to resist decomplexation and release of siRNA before they reach the cytosol of target cells. Therefore, maintaining a balanced complex stability is important to successful transfection and subsequent knockdown of the desired target.

Figure 4 showed that nanoparticle stability increased with increasing P′/N ratio and N/P ratio. Incubation of nanoparticle with PVSK for 1 h resulted in minimal release of siRNA from particles formed with N/P ratios of 4 and 8 at various P′/N ratios. However, the differences began to emerge at a later time point (5 h after incubation). The intensity of released siRNA bands were easily detected, and their intensity decreased with increasing P′/N ratio. Moreover, the observed intensity of migratory siRNA band at N/P of 8 was slightly weaker than that at N/P of 4. These data gave comparative stabilities of various nanoparticles prepared with different N/P and P′/N ratios, confirming that both PEG-b-PPA and TPP contributed to the stability of nanoparticles.

Transfection and Knockdown Efficiency of PPA-*b*-PPA/siRNA Nanoparticles

The knockdown efficiency of PPA-*b*-PPA/siRNA nanoparticles *in vitro* was assessed in two different types of cells, human epithelial cervical cancer cells (HeLa) and human

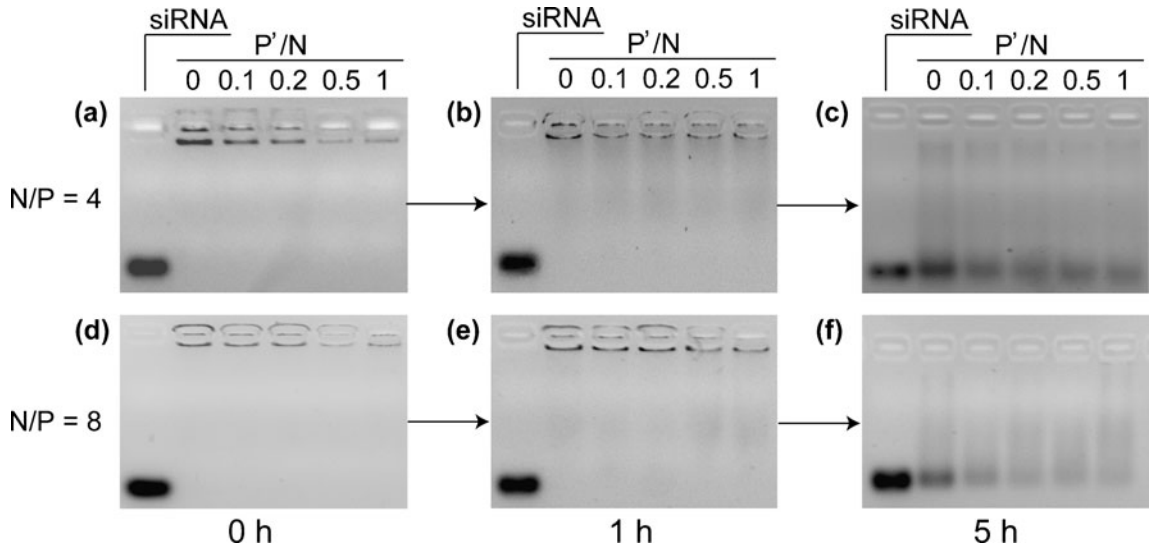

Fig. 4 Gel retardation assay of complexation efficiency for siRNA at various P′/N ratios for N/P ratios of 4 and 8, respectively. Nanoparticles prepared at various conditions were incubated with PVSK for 1 and 5 h at 37°C at a molar ratio of sulfate groups in PVSK to phosphate groups in siRNA of 5.

retinal pigment epithelial cells (D407) in the absence (Fig. 5a) and presence of serum (Fig. 5b). In this experiment, HeLa and D407 cells were transiently transfected respectively with the two kinds of reporter genes P-Luc and R-Luc, followed by the treatment with nanoparticles prepared at different P′/N ratios (0 to 1.0) with siRNA against P-Luc. The expression level of R-Luc was used as an internal reference for the initial transgene expression level. After transfection period of 44 h, the inhibition of P-Luc expression was evaluated by measuring the relative expression ratio of P-Luc/R-Luc at a concentration of 100 nM siRNA.

Although PEG-*b*-PPA/siRNA complexes without TPP failed to show distinct measurement of nanoparticles in DLS, they mediated an average of 24% and 58% knockdown efficiency in HeLa cells and 40% to 56% in D407 cells in serum-free medium at N/P ratios of 4 and 8, respectively. TPP-crosslinked nanoparticles resulted in higher knockdown efficiencies at both N/P ratios in both cell lines. As the P′/N ratio increases, the gene knockdown efficiency increased gradually. At N/P ratio of 4, the knockdown efficiency reached the plateau of ca. 60% at P′/N ratio of 0.5 in HeLa cells and the highest knockdown efficiency of ca. 60% at P′/N ratio of 1.0 in D407 cells (Fig. 5a). The knockdown efficiency was higher at N/P of 8 and reached ca. 75% of knockdown efficiency in both types of cells.

Interestingly, however, when the transfections were conducted in 10% serum-containing medium, the knockdown efficiency of PEG-*b*-PPA/siRNA complexes without TPP stabilization was significantly reduced compared to that obtained in serum-free condition (Fig. 5b). The knockdown efficiency for N/P ratio of 4 was 10–12%, and 23–34% at N/P ratio of 8 in both cell lines. In contrast, the knockdown efficiency of TPP-crosslinked nanoparticles was maintained or slightly enhanced as compared to that obtained in serum-free medium transfection. As the P′/N ratio increased, the gene knockdown efficiency maintained a similar level in HeLa cells and moderately increased in D407 cells. At N/P ratio of 4, the knockdown efficiency reached the plateau of ca. 50% in Hela cells and a maximum of 70% in D407 cells. Higher knockdown efficiency was obtained at N/P of 8 for both cell lines, with 75% to 80% knockdown efficiency obtained in HeLa cells and D407 cells, respectively, at P′/N ratio of 1.

Cytotoxicity of PEG-*b*-PPA/siRNA Nanoparticles

The potential cytotoxicity of PEG-*b*-PPA/siRNA nanoparticles was assessed in HeLa cells and D407 cells under the transfection conditions. The cell viability was determined by WST assay using water-soluble tetrazolium salt (Fig. 6). Nearly 100% of cell viability was observed for all transfection conditions in HeLa cells, and over 90% of cell viability of D407 cells was observed under the same conditions. There was no significant difference in cell viability observed between nanoparticles prepared with and without TPP crosslinking. Similar cytotoxicity results were obtained under serum-free transfection condition (data not shown). These results demonstrated that the addition of TPP into nanoparticle assemblies did not influence their cytotoxicity.

DISCUSSION

Compacting siRNA with polymeric carrier into distinct, small and stable nanoparticles has been challenging due to the much lower molecular weight and condensation ability of siRNA as compared with plasmid DNA. Particle size and size distribution are important determinants for successful

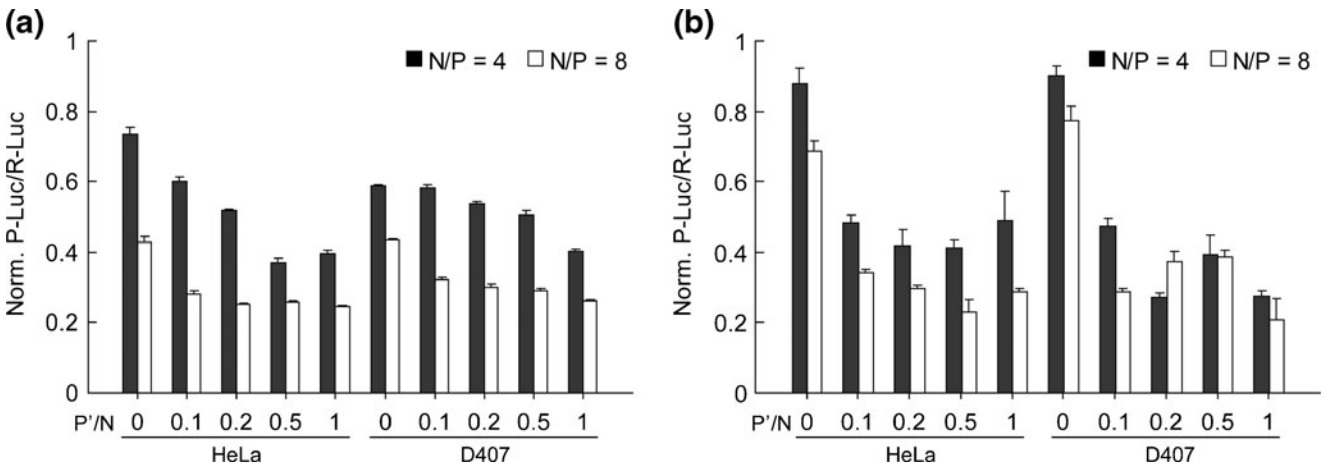

Fig. 5 Gene silencing efficiency mediated by PEG-PPA/siRNA/TPP ternary nanoparticles at various P′/N ratios for N/P ratios of 4 and 8 in HeLa and D407 cells in the absence (**a**) and presence (**b**) of 10% serum. A siRNA dose of 100 nM was used in all transfection groups. Values are expressed as Mean ± SEM ($n = 4$).

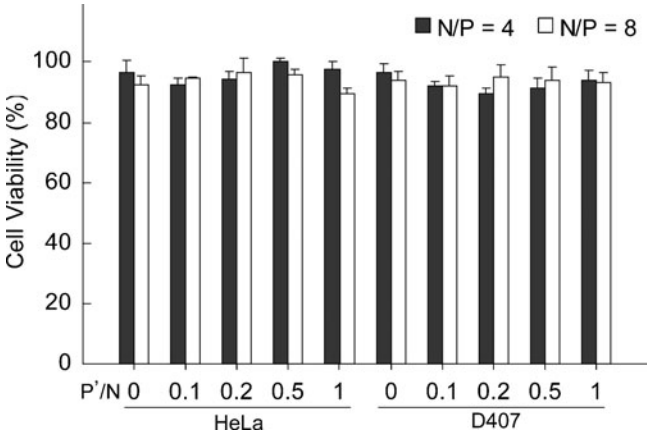

Fig. 6 Viability of HeLa and D407 cells transfected with PEG-PPA/siRNA/TPP ternary nanoparticles in 10% serum-containing medium under the conditions described in Fig 5. Values are expressed as Mean ± SEM ($n = 4$).

gene transfection and transport properties *in vivo*. It has been reported that particles in the nanometer-sized range have a relatively higher cellular uptake and intracellular transport compared to microsized particles (30–33). Here we proposed a convenient method to enhance the condensation between PEG-*b*-PPA and siRNA. Smaller and more uniform nanoparticles were formed with relatively low concentration of TPP at lower N/P ratios. The major advantages of TPP as a stabilization crosslinker are its low toxicity and the convenience of simply mixing TPP and siRNA solution before complexing with PEG-*b*-PPA. In addition, the inclusion of TPP did not interfere with the complexation between PEG-*b*-PPA and siRNA.

Although PEG-*b*-PPA and siRNA formed complexes at N/P ratios of 4 and 8, particles were irregularly shaped with wide size distribution. The addition of TPP drastically improved the condensation efficiency, forming spherical nanoparticles with small and distinct sizes at P′/N ratio as low as 0.2. The mechanism of enhanced condensation is likely through intermolecular electrostatic interaction, due to the multivalent anionic nature of TPP. Mixing PEG-*b*-PPA with TPP only (without siRNA) at a P′/N ratio between 0.1 and 1.0 also formed particles with average size ranging from 180 to 200 nm and a PDI of ca. 0.3 (data not shown). This confirms that TPP has the ability to condense polycations and form nanoparticles through electrostatic interaction. These particles exhibited much bigger size and PDI as compared with PEG-*b*-PPA/siRNA/TPP nanoparticles. Together with the observation of unimodal distribution of PEG-*b*-PPA/siRNA/TPP nanoparticles, these results indirectly confirmed that TPP participated in forming the ternary nanoparticles, rather than forming separate populations of PEG-*b*-PPA/TPP and PEG-*b*-PPA/siRNA particles.

Another advantage of the PEG-*b*-PPA/siRNA/TPP nanoparticle system is the tunable stability. The complex stability of the ternary nanoparticles was found to be dependent on N/P and P′/N ratios. The stabilization effect of TPP increased with P′/N ratio and was more pronounced at lower N/P ratio. In general, the PEG-*b*-PPA/siRNA/TPP ternary nanoparticles were smaller and more stable at higher N/P and P′/N ratios. Based on the required stability for different gene knockdown applications, it may be possible to fine-tune the stability of the ternary nanoparticles to maintain sufficient stability for nanoparticles to transport to target cells, escape endolysosomal compartment, reach the cytosol of target cells, and allow intracellular release of siRNA in physiological ionic strength and in the presence of polyelectrolytes. On the other hand, siRNA integrity in serum condition was less dependent on all N/P and P′/N ratios tested. Resistance of siRNA to enzymatic degradation is not the major reason for enhanced knockdown efficiency, because complexes formed without TPP crosslinking showed similar protection to siRNA in 50% FBS-containing medium. This result was similar to that reported in the case of PEG-*b*-polylysine/siRNA complexes (18).

The co-condensation of TPP also significantly modulated the nanoparticle surface charge. The ζ-potential of the ternary nanoparticles reduced drastically to neural at a P′/N ratio of 0.5. This may significantly impact the *in vivo* nanoparticle transport and stability, as positively charged nanoparticles are prone to opsinization and passive adsorption with abundant negatively charged serum proteins, leading to particle aggregation and uptake by macrophages. This hypothesis remains to be tested in an *in-vivo* transfection study in the near future.

The improved stability of the ternary nanoparticle systems correlated well with their enhanced gene knockdown efficiency over PEG-*b*-PPA/siRNA complexes. Although the enhancement effect was less pronounced at higher N/P ratio, the TPP-crosslinked nanoparticles showed the highest transfection and transgene knockdown efficiency for all P′/N and N/P ratios tested. More importantly, the knockdown efficiency of PEG-*b*-PPA/siRNA complexes in serum-containing medium was significantly reduced as compared to that obtained in serum-free transfection in both cell lines, whereas the efficiency was maintained or enhanced for TPP-crosslinked nanoparticles in serum-containing medium in both cell lines and at both N/P ratios. Given that TPP-crosslinked nanoparticles at higher P′/N ratios showed neutral or negative surface charges, which likely decreased nanoparticle binding with cell surface, hence reducing cellular uptake, the higher knockdown efficiency of ternary nanoparticles may primarily be attributed by the more compact size and increased complex stability of nanoparticles. Both factors may favor particle uptake and the protection of siRNA during endocytosis and in endolysosomal compartment, eventually leading to improved gene knockdown activity. More

detailed mechanistic understanding of the intracellular trafficking TPP-crosslinked nanoparticles as a function of P′/N ratio remains to be investigated.

Finally, this stabilization strategy for PEG-*b*-PPA/siRNA complexes has minimal side effect, as the cytotoxicity profile of the ternary nanoparticles was the same as PEG-*b*-PPA/siRNA complexes without TPP addition. This is consistent with the low toxicity profile of TPP, which is an FDA direct food additive (21 CFR 173.310) and is on the GRAS (generally recognized as safe) list.

CONCLUSIONS

In this study, we demonstrated that co-condensation with TPP was a safe and effective approach to improve the complex stability and gene silencing efficiency of PEG-*b*-PPA/siRNA nanoparticles. By simply mixing TPP with siRNA before condensing with PEG-*b*-PPA, spherical ternary nanoparticles with smaller size and narrow distribution were obtained. These ternary nanoparticles showed improved complex stability in salt and serum-containing medium and against polyanion exchange reaction. The stability of ternary nanoparticles increased with increasing P′/N and N/P ratios. The release of encapsulated siRNA was observed following incubation with polyanions. The improved stability correlated well with the enhanced transfection and gene knockdown efficiency of the ternary nanoparticles. The knockdown efficiency of TPP-crosslinked nanoparticles was much higher than PEG-*b*-PPA/siRNA complexes in serum-containing medium. These results highlight the TPP-co-condensation as a promising strategy to improve the efficiency of polymer/siRNA nanoparticle-mediated gene knockdown approaches.

ACKNOWLEDGMENTS

The authors thank Dr. James F. Dillman III and Dr. Albert L. Ruff at the Cell and Molecular Biology Branch, US Army Medical Research Institute of Chemical Defense, and Dr. Xuan Jiang at Department of Materials Science and Engineering, Johns Hopkins University, for discussions throughout the study. We thank Dr. Noriko Esumi for providing D407 cells. This study was supported by US Army Defense Threat Reduction Agency through the Grant W81XWH-10-2-0053.

REFERENCES

1. Kim DH, Behlke MA, Rose SD, Chang MS, Choi S, Rossi JJ. Synthetic dsRNA Dicer substrates enhance RNAi potency and efficacy. Nat Biotechnol. 2005;23:222–6.
2. Elbashir SM, Lendeckel W, Tuschl T. RNA interference is mediated by 21-and 22-nucleotide RNAs. Genes Dev. 2001;15:188–200.
3. Elbashir SM, Harborth J, Lendeckel W, Yalcin A, Weber K, Tuschl T. Duplexes of 21-nucleotide RNAs mediate RNA interference in cultured mammalian cells. Nature. 2001;411:494–8.
4. Grimmand D, Kay MA. Therapeutic application of RNAi: is mRNA targeting finally ready for prime time? J Clin Investig. 2007;117:3633–41.
5. Manoharan M. RNA interference and chemically modified small interfering RNAs. Curr Opin Chem Biol. 2004;8:570–9.
6. Guo PX, Coban O, Snead NM, Trebley J, Hoeprich S, Guo SC, *et al*. Engineering RNA for targeted siRNA delivery and medical application. Adv Drug Deliv Rev. 2010;62:650–66.
7. Nothisen M, Kotera M, Voirin E, Remy JS, Behr JP. Cationic siRNAs provide carrier-free gene silencing in animal cells. J Am Chem Soc. 2009;131:17730–1.
8. Eguchiand A, Dowdy SF. siRNA delivery using peptide transduction domains. Trends Pharmacol Sci. 2009;30:341–5.
9. Frohlichand T, Wagner E. Peptide- and polymer-based delivery of therapeutic RNA. Soft Matter. 2010;6:226–34.
10. David S, Pitard B, Benoit JP, Passirani C. Non-viral nanosystems for systemic siRNA delivery. Pharmacol Res. 2010;62:100–14.
11. Jeong JH, Kim SW, Park TG. Molecular design of functional polymers for gene therapy. Prog Polym Sci. 2007;32:1239–74.
12. Khurana B, Goyal AK, Budhiraja A, Arora D, Vyas SP. siRNA delivery using nanocarriers—an efficient tool for gene silencing. Curr Gene Ther. 2010;10:139–55.
13. Mok H, Lee SH, Park JW, Park TG. Multimeric small interfering ribonucleic acid for highly efficient sequence-specific gene silencing. Nat Mater. 2010;9:272–8.
14. Bolcato-Bellemin AL, Bonnet ME, Creusatt G, Erbacher P, Behr JP. Sticky overhangs enhance siRNA-mediated gene silencing. Proc Natl Acad Sci USA. 2007;104:16050–5.
15. Raemdonck K, Van Thienen TG, Vandenbroucke RE, Sanders NN, Demeester J, De Smedt SC. Dextran microgels for time-controlled delivery of siRNA. Adv Funct Mater. 2008;18:993–1001.
16. Tamura A, Oishi M, Nagasaki Y. Enhanced cytoplasmic delivery of siRNA using a stabilized polyion complex based on PEGylated nanogels with a cross-linked polyamine structure. Biomacromolecules. 2009;10:1818–27.
17. Li J, Chen YC, Tseng YC, Mozumdar S, Huang L. Biodegradable calcium phosphate nanoparticle with lipid coating for systemic siRNA delivery. J Control Release. 2010;142:416–21.
18. Matsumoto S, Christie RJ, Nishiyama N, Miyata K, Ishii A, Oba M, *et al*. Environment-responsive block copolymer micelles with a disulfide cross-linked core for enhanced siRNA delivery. Biomacromolecules. 2009;10:119–27.
19. Jiang X, Dai H, Ke CY, Mo X, Torbenson MS, Li ZP, *et al*. PEG-b-PPA/DNA micelles improve transgene expression in rat liver through intrabiliary infusion. J Control Release. 2007;122:297–304.
20. Jiang X, Zheng Y, Chen HH, Leong KW, Wang TH, Mao HQ. Dual-sensitive micellar nanoparticles regulate DNA unpacking and enhance gene-delivery efficiency. Adv Mater. 22:2556–60.
21. Allen TM, Hansen C, Martin F, Redemann C, Yauyoung A. Liposomes containing synthetic lipid derivatives of poly(ethylene glycol) show prolonged circulation half-lives *inviv*o. Biochim Biophys Acta. 1991;1066:29–36.
22. Klibanov AL, Maruyama K, Torchilin VP, Huang L. Amphipathic polyethyleneglycols effectively prolong the circulation time of liposomes. FEBS Lett. 1990;268:235–7.
23. Calvo P, RemunanLopez C, VilaJato JL, Alonso MJ. Chitosan and chitosan ethylene oxide propylene oxide block copolymer

nanoparticles as novel carriers for proteins and vaccines. Pharm Res. 1997;14:1431–6.
24. Calvo P, RemunanLopez C, VilaJato JL, Alonso MJ. Novel hydrophilic chitosan-polyethylene oxide nanoparticles as protein carriers. J Appl Polym Sci. 1997;63:125–32.
25. Park JH, Saravanakumar G, Kim K, Kwon IC. Targeted delivery of low molecular drugs using chitosan and its derivatives. Adv Drug Deliv Rev. 2010;62:28–41.
26. Mao SR, Sun W, Kissel T. Chitosan-based formulations for delivery of DNA and siRNA. Adv Drug Deliv Rev. 2010;62:12–27.
27. Nasti A, Zaki NM, de Leonardis P, Ungphaiboon S, Sansongsak P, Rimoli MG, *et al.* Chitosan/TPP and chitosan/TPP-hyaluronic acid nanoparticles: systematic optimisation of the preparative process and preliminary biological evaluation. Pharm Res. 2009;26:1918–30.
28. Bakeev KN, Izumrudov VA, Kuchanov SI, Zezin AB, Kabanov VA. Kinetics and mechanism of interpolyelectrolyte exchange and addition-reactions. Macromolecules. 1992;25:4249–54.
29. Katayoseand S, Kataoka K. Water-soluble polyion complex associates of DNA and poly(ethylene glycol)-poly(L-lysine) block copolymer. Bioconjug Chem. 1997;8:702–7.
30. Ishida O, Maruyama K, Tanahashi H, Iwatsuru M, Sasaki K, Eriguchi M, *et al.* Liposomes bearing polyethyleneglycol-coupled transferrin with intracellular targeting property to the solid tumors *in vivo*. Pharm Res. 2001;18:1042–8.
31. Litzinger DC, Buiting AMJ, Vanrooijen N, Huang L. Effect of liposome size on the circulation time and intraorgan distribution of amphipathic poly(ethylene glycol)-containing liposomes. Biochim Biophys Acta, Biomembr. 1994;1190:99–107.
32. Uchiyama K, Nagayasu A, Yamagiwa Y, Nishida T, Harashima H, Kiwada H. Effects of the size and fluidity of liposomes on their accumulation in tumors—a presumption of their interaction with tumors. Int J Pharm. 1995;121:195–203.
33. Akitaand H, Harashima H. Advances in non-viral gene delivery: using multifunctional envelope-type nano-device. Expert Opin Drug Deliv. 2008;5:847–59.